Electrochemical, Structural and Nano Tribological Behavior of Ni-W-PTFE Nanocomposite Coatings Prepared by Tartrate Bath

Amir Farzaneh[1], Mir Ghasem Hosseini[2,], Shahin Khameneh Asl[1], Omer Mermer[3,*]*

[1] Department of materials engineering, Faculty of Mechanical Engineering, University of Tabriz, Tabriz, Iran,
[2] Department of Physical Chemistry, Electrochemistry Research Laboratory, University of Tabriz, Tabriz, Iran,
[3] Department of Electrical and Electronic Engineering, Ege University, 35100, İzmir, Turkey
[*]E-mail: mg-hosseini@tabrizu.ac.ir, omer.mermer@ege.edu.tr

A tartrate nickel plating bath has been used to prepare nickel- tungsten (Ni-W) dispersed PTFE composite coatings with four different PTFE contents (0, 4, 8 and 20 gl^{-1}). The coatings are characterized using of Field-Emission Scanning Electron Microscopy (SEM), Energy Dispersive X-ray Analysis (EDAX) and X-ray Diffractometry (XRD). XRD results indicate that the PTFE particle changed the surface texture significantly. The nano tribological behavior of the nano composite coating was estimated by contact mode of AFM. Electrochemical performance of the nanocomposite depositions was evaluated using potentiodynamic polarization and electrochemical impedance spectroscopy (EIS). The results show that the Ni-W/PTFE nanocomposite films exhibit better electrochemical and tribological performance   than the Ni-W coating. The corrosion rate and surface roughness decreased about 50 and 5 times less than bare coating in optimum condition 8 gl^{-1} PTFE.

1. INTRODUCTION

During recent decade there are significant advances in technology, so it demands new types of materials by high reliability, long life and service safety in highly aggressive environments[1]. Among the various types of materials, metal matrix composite films have been attracting keen interest during last several decades, because of their unique properties such as magnetic, electrochemical, mechanical, and chemical properties [2-5]. The metal composite coatings can be fabricated most commonly by electro- deposition method. Electrodeposition is an easy one- step technique in which can be co-

deposited various ceramic and polymer particle with micron and submicron size to form monolithic with appreciable thickness and controlled shape[3, 4, 6, 7].

Reinforcement of solid particle could improve composite coatings abrasion resistance, hardness and thermal stability[8, 9]. This could also lower their friction coefficient, and change their adhesion properties. Soft solid lubricants such as polytetrafluoroethylene (PTFE) and MoS_2 could improve tribological resistant by reducing friction coefficient [9-11]. Electrodeposited Ni-PTFE (polytetrafluoroethylene) composite film have been of attract great interest for industrial application, because of their good water repellency, solid lubrication and corrosion performance [12-14].

During last decade there are considerably research about Ni-PTFE composite coating and their wear and corrosion behavior. Binary Alloys like Ni − W or Ni − Mo because of their excellent magnetic properties, strength and heat resistance and ideal wear and corrosion resistance are the most attractive candidate for bulk coating materials[11, 15]. Recently, Sangeetha and et al reported a study about pulse electrodeposition of self-lubricating Ni-W/PTFE [23-24]. To the best of our knowledge this is the only report about Ni-W/PTFE coating. However, this report provided limited information on the deposition process and characterization of the composite coatings without pulse electrodeposition. But researches about the alloy Ni base matrix with PTFE nanoparticles are still needed. There is no comprehensive research about effect of PTFE nanoparticles on corrosion properties of Ni–W/PTFE composite coating.

Herein, we investigate the electrodeposition of the composite coatings from a tartrate nickel plating. It is also demonstrated the effects of PTFE nanoparticle concentrations on the properties of the nanocoatings. Moreover, electrochemical, structural and nano tribological behavior of Ni–W-PTFE composite coatings were characterized in details.

2. MATERIALS AND METHODS

2.1. Preparation of composite coatings

The copper sheet with 10×10 mm^2 size has been choosing as a substrate. Before the electrodeposition of nickel nanocomposite coatings, the Cu substrate were polished by successive emery papers up to 2000 and then degreased in a 30% NaOH solution for 5 min, washed with distilled water, and dried in air. Thereafter, the substrates were washed in distilled water and activated in 10% H_2SO_4 for 60 s at room temperature and then subjected to the electrodeposition process.

Ni-W coatings with different concentration of PTFE (0, 4, 8 and 20 gl^{-1}) was carried out using nickel sulfate ($NiSO_4 \cdot 6H_2O$) as a source of nickel, Potassium sodium tartrate tetra hydrate ($C_4H_4KNaO_6 \times 4\ H_2O$) as complexing agent, Sodium tungstate ($Na_2WO_4 \times 2\ H_2O$) as a source of tungsten. For improve dispersion of second phase (PTFE particles (Mecrk, 20-200nm)), sodium dodecyl benzene sulfonate ($C_{18}H_{29}NaO_3S$, 99.99%) was used as surfactant. During the plating, the electrolyte was agitated using a magnetic stirrer at 350 rpm; the pH and temperature of the electrolyte were maintained at ±0.2 units and ±0.1 °C, respectively. Table 1 listed the details of electrodeposition bath composition and operating conditions.

Table 1. Electrodeposition bath composition and operating conditions

Bath Composition		Operating conditions	
Nickel sulfate (g l^{-1})	20	pH	5± 0. 2
Sodium tungstate (g l^{-1})	65	Deposition temp. (°C)	45± 2
Potassium sodium tartrate (g l^{-1})	85	Bath Vol. (ml)	200
Surfactant (g l^{-1})	0.001	PTFE content (g l^{-1})	0, 4, 8, 20

2.2 Characterization of composite coatings

Field- emission scanning electron microscope (SEM) MIRA3 FEG-SEM Tescan) equipped with energy dispersive X-ray spectroscopy (EDS) have been used for characterization of surface morphology and composition. Phase composition was determined using X-ray diffraction analysis (Bruker D2 Phaser, Cu Kα radiation). Surface topography, roughness and friction were determined in air in the contact mode with a Contact AFM commanded by a Nanosurfe Atomic Force Microscope (AFM).

3.5 wt. % NaCl solution have been used as a corrosive medium. The samples were first immersed into solution for about 1500 s to stabilize the open-circuit potential. Electrochemical and corrosion performance of the nanocomposite films were measured using potentiostat/Galvanostat model 263A EG&G Princeton Applied Research (PAR) and a classical three electrodes cell with a platinum electrode as counter electrode, saturated calomel electrode (SCE) as reference electrode and the samples with an exposed area of 1cm^2 as working electrode. The potentiodynamic polarization curves and open-circuit potential (EOCP) were recorded using a constant voltage scan rate of 1 mVs^{-1}. Electrochemical impedance spectroscopy (EIS) experiments were done in the frequency range of 100 kHz-10 mHz and the perturbation amplitude was 5 mV.

3. RESULTS AND DISCUSSION

3.1. Surface morphology and chemical composition

The Ni-W-PTFE composite coatings with four concentrations (0, 4, 8 and 20 gl^{-1}) have been developed on the copper substrate. Fig. 1 depicts the SEM images of the Ni –W and Ni–W/PTFE composite coatings. As shown in the Figure, the sample with 4 and 8 gl^{-1} PTFE have a smooth and compact surface. This structure is optimized in 8 gl^{-1} PTFE, but by increasing the PTFE concentration, the coating morphology has been changed and some defected shape has been appeared and nodule size has been increased. This behavior was also confirm by our previous work [16].

Fig. 2 and table 2 illustrate the EDS results of chemical composition analysis of the nano composite coatings. The results indicate that Ni-W is mainly composed of Ni 76.57wt. % and 23.43wt. %. of W. By addition of PTFE to the coating bath, the concentration of Ni decrease in the final coating, but the W concentration almost is stable. According to the PTFE chemical formula, the content of F is

the symbol of the PTFE material in the deposition. The F content in the film can be estimated by the EDS analysis. The result in Table 2 shows that the F content in the coating increased by increasing the PTFE concentration in the bath. Therefore, it can be conclude that the PTFE percentage in the deposition increased by increasing PTFE concentration in the electrolytes.
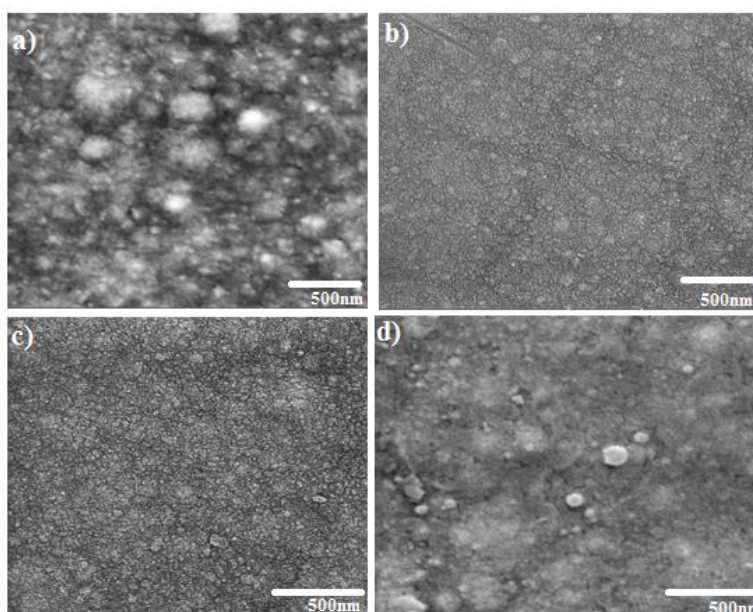
Figure 1. SEM images of the Ni-W-PTFE a) 0 g 1^{-1} b) 4 g 1^{-1} c) 8 g 1^{-1} and d) 20 g 1^{-1}.
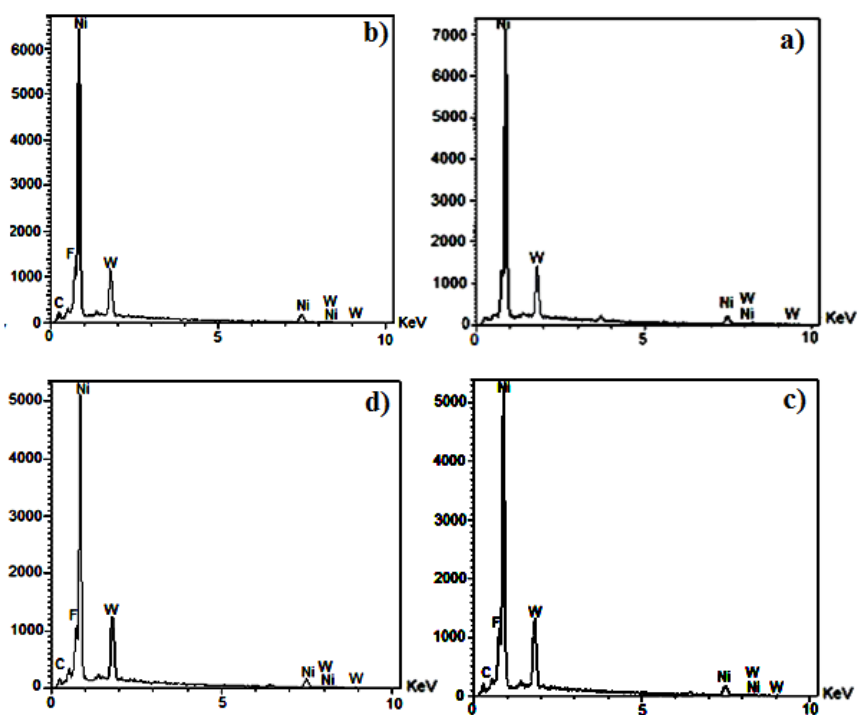
Figure 2. EDS images and elemental composition of Ni-W-PTFE a) 0 g 1^{-1} b) 4 g 1^{-1} c) 8 g 1^{-1} and d) 20 g 1^{-1} coatings.

Table 2. EDS chemical composition analysis results for various Ni-W-PTFE coatings.

	Ni (%wt)	W (%wt)	F (%wt)	C (%wt)
Ni-W-PTFE (0 g l^{-1})	76.57	23.43	-	-
Ni-W-PTFE (4 g l^{-1})	69.78	22.38	1.7	6.14
Ni-W-PTFE (8 g l^{-1})	66.38	23.91	2.64	7.07
Ni-W-PTFE (20 g l^{-1})	64.22	24.77	1.49	7.45

3.2 XRD measurement

The XRD results of prepared samples with different plating conditions have been shown in Fig. 3. The XRD patterns indicate the main peaks corresponding to (111), (200) and (220) crystallographic planes. A new amorphous shape pattern appeared which signifies the presence of a PTFE phase in the coating. By adding PTFE to the electrolyte, the peaks intensity changed and broadening have been occurred. At higher concentration of PTFE, this trend can be seen more effectively and the crystallinity of the coatings with 8 and 20 gl^{-1} PTFE are lower than the other coatings. In general, Ni-W-PTFE deposits have mixed crystalline and amorphous microstructures. As it shown the intensity of the diffraction peaks of Ni-W/PTFE films decreased by increasing PTFE concentration in electrolyte. The lowest intensity obtained in 8 gl^{-1} PTFE. The crystalline size of the coating have been calculated using the Scherrer formula[17]:

$$D = \frac{0.9\lambda}{\beta \cos\theta}$$

where D is the grain size , λ is the wavelength, β is the peak width and θ is the peak angle. This equation shows that broadening of peaks (β) is inversely proportional to the grain size (D)[18]. Fig. 4 depicts the average crystalline size of nanocomposite coatings. Results show that adding PTFE decreases crystal size in prepared coatings until 8 gl^{-1} and in 20 gl^{-1} the crystalline size increased.

The surface texture changes regards to the different crystal planes were estimated using the 'Relative Texture Coefficient' (RTC). This method can be used for quantify crystal planes in electrodeposited metal-based coatings [19]. The Relative Texture Coefficient or RTC (hkl) for a (hkl) crystal plane is defined as:

$$RTC_{(hkl)} = 100 \times \left(\frac{\frac{I_{(hkl)}}{I^0_{(hkl)}}}{\sum_1^3 \frac{I_{(hkl)}}{I^0_{(hkl)}}} \right)$$

where I(hkl) are the relative intensities of the (hkl) reflection, I^0(hkl) is the intensity of the reflection for the same crystal plane in a standard Ni powder sample[20]. The three basic lines of the total reflection lines are considered (111), (200) and (220) for this estimation. Fig. 5 illustrate calculated RTC (hkl) values for all the Ni crystal planes in each 2θ scan. According the results, the

RTC (200) decreased by increasing PTFE concentration and RTC (220) and (111) are increased. The sample with 8 gl^{-1} PTFE has maximum change in crystal orientation. The (220) plan percent increase up to 39% in this sample. This changings in RTC value can be explained the value of the relative texture coefficient of each crystalline orientation. According to the Aruna and et all.[19], when the charged particles arrive at the cathode surface, they are loosely adsorbed or partially submerged onto the growing nickel grains. This phenomena have been affected the surface texture, grain and crystalline orientation. The same trend occurs in our results and PTFE changed the surface crystal orientation. The RTC variance can be attributed to changing surface morphology in nano composite coating.
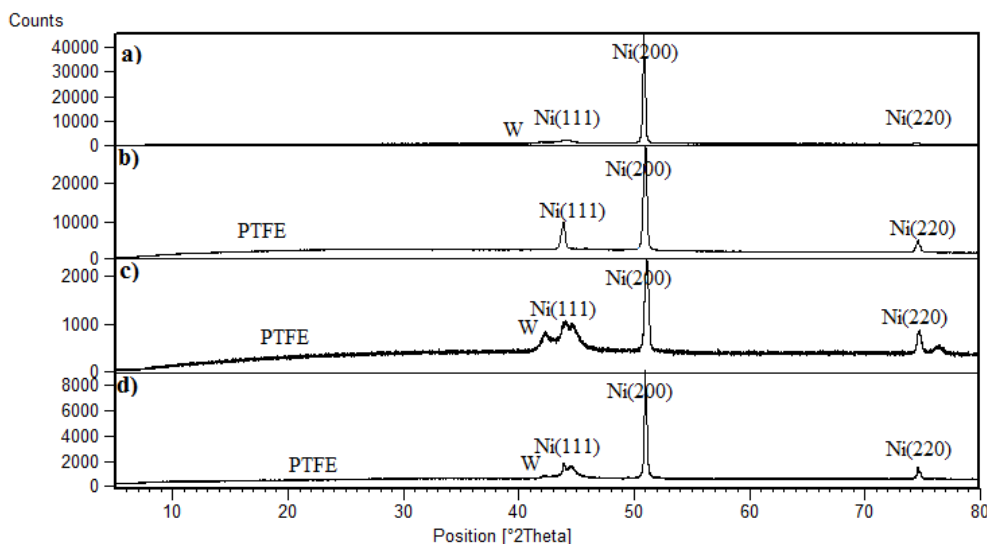
Figure 3. X ray Diffractograms of the Ni-W-PTFE a) 0 g 1^{-1} b) 4 g 1^{-1} c) 8 g 1^{-1} and d) 20 g 1^{-1} coatings.
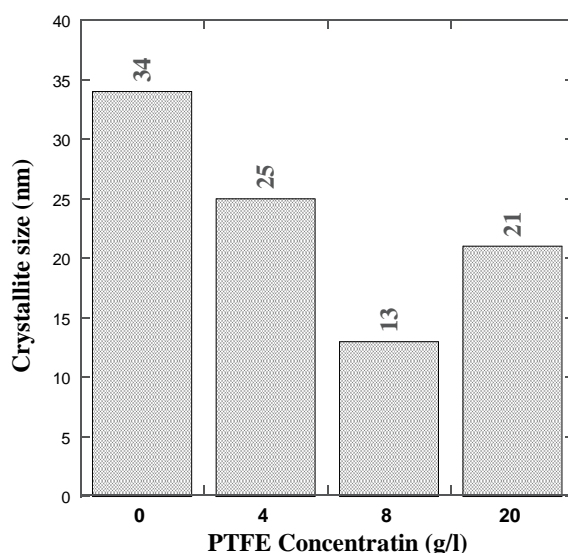
Figure 4. Crystalline size of prepared samples as a function of PTFE concentration.
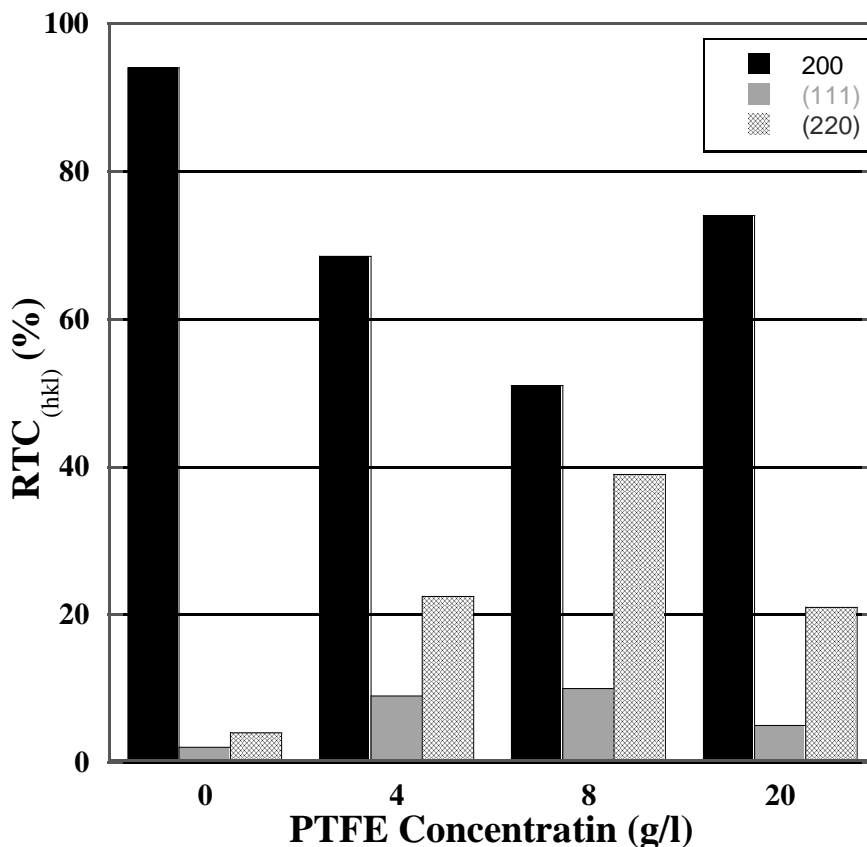
Figure 5. RTC (hkl) results for different crystal planes observed in prepared samples as a function of PTFE concentration.

3.3 Nano-Tribological performance

Surface topography (3D AFM morphological images) and surface roughness factor (R_a) of prepared coatings have been shown in the Fig. 6 and 7, respectively. As shown in Fig. 6, the surface morphology significantly changed by addition of PTFE in the deposition bath. The size of surface peaks and valleys decrease and the nano range surface roughness have been appeared. Regard to the SEM results the same trend appear here and the optimum and smallest size have been found in 8 gl^{-1} PTFE. The surface roughness results confirm that the 8 gl^{-1} PTFE sample is optimum condition for surface homogeneity and has the lowest surface roughness compare to the other samples. The friction behavior of prepared samples has been evaluated by AFM in contact mode. The obtained results have shown in Fig. 8. As seen in the figure, the coating with 8 g l^{-1} PTFE shows the lowest friction force in comparison with other conditions. The PTFE known as a self-lubricant agent[21] and this composition in the coating decrease the friction force. Here also the sample with 8 gl^{-1} PTFE has a lowest friction force by stable feature with compare other samples.

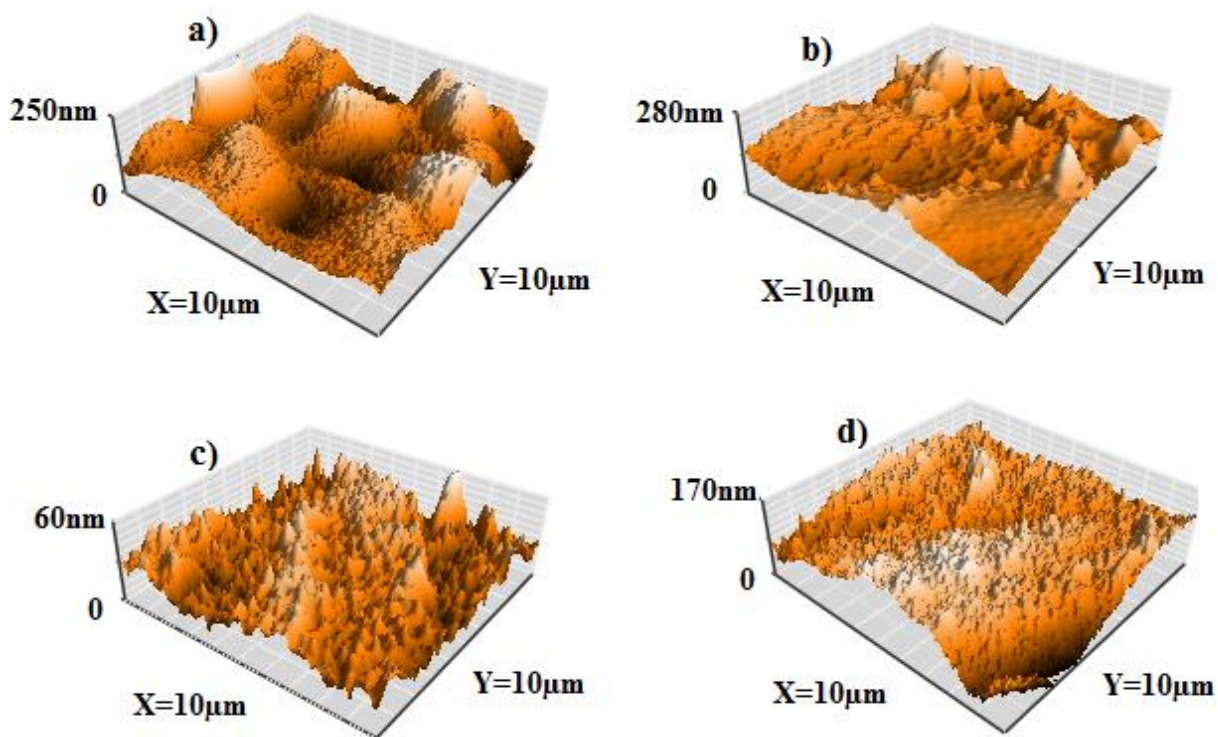**Figure 6.** AFM morphological images of Ni–W-PTFE a) 0 g 1^{-1} b) 4 g 1^{-1} c) 8 g 1^{-1} and d) 20 g 1^{-1} coatings.
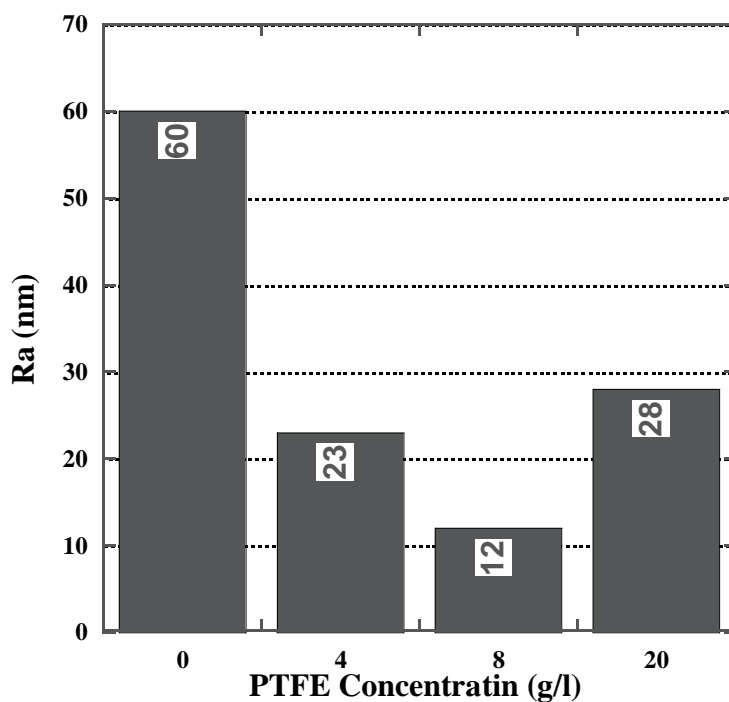

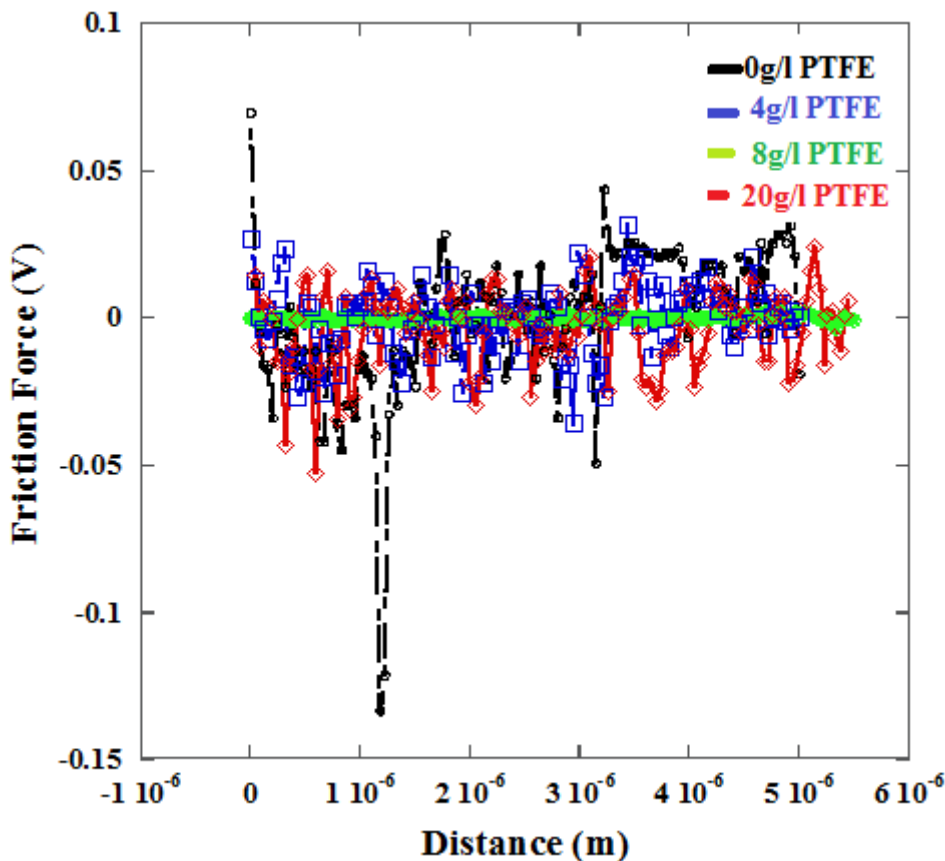**Figure 7.** R_a roughness factor of prepared coatings.

**Figure 8.** AFM Friction force data of prepared coatings.

3.4 Corrosion properties

The corrosion behavior of different coating has been evaluated by two methods. The first method is potentiodynamic polarization method. Fig. 9 illustrates the open circuit polarization (OCP) behavior of coating samples. As shown in the figure, the OCP changes in the coating with 8 g l^{-1} is lower than other coatings and this shows the higher homogeneity of this condition compare with other samples. Also the PTFE shifted their potential to the positive amount resulting that the PTFE make the coating nobler than bare coatings. This large potential shift to the passive region in Ni-W-PTFE nanocomposite coatings may be related to their microstructures. According to the SEM and AFM images, the surface morphology of Ni-W-PTFE 8gl^{-1} coating has a suitable micro-nano rough surface. The potentiodynamic polarization graphs have been illustrated in Fig. 10. This figure shows the resulting current (in log scale) versus corrosion potential. Corrosion potential, E$_{corr}$, has been obtained directly from experimental polarization curve (Fig. 10) whereas the corrosion current, i$_{corr}$, is obtained from a Tafel plot by extrapolating the linear portion of the curve as shown in Fig. 10. The calculated corrosion current (i$_{corr}$) and corrosion potential (E$_{corr}$) values from the Tafel polarization curves are also listed in Table 3. The Ni-W coating shows a passivation phenomenon, that is indicated the formation of a thin passive film. The plots of the Ni–W-PTFE coatings have a sharp slope and no stabilized current in anodic area. This trends were also observed by Wang et al[22]. They explained this behavior by structure transformation in the Ni-W/SiO2 nanocomposite coatings. According to

our XRD results, the concentration PTFE nanoparticles changed the crystal orientation and grain boundary of the composites. Therefore, the Ni-W-PTFE composite coating did not have a passivation behavior like Ni-W coatings because of crystallity and surface texture differences. The potentiodynamic polarization results confirm that the corrosion resistance of the Ni-W-PTFE was increased with increasing the concentration of PTFE nanoparticles until 8 gl^{-1}. Szeptycka et.al. reported that the structure of the coatings influenced the percentage increase of the corrosion resistance [12]. The same trend was also observed in our result. It may be inferred that inclusion of PTFE nanoparticles which probably acted as an internal physical barrier, thus have been improved the anticorrosion property of the Ni-W-PTFE composite coating. According to the Sangeetha et. al. [23], reinforcement of PTFE nanoparticle covered the cracks and holes of the Ni-W alloy matrix and hence the self-lubricating PTFE polymer layer has enhanced the anticorrosion property of the nanocomposite coatings. Our results are significantly agreement with literature.
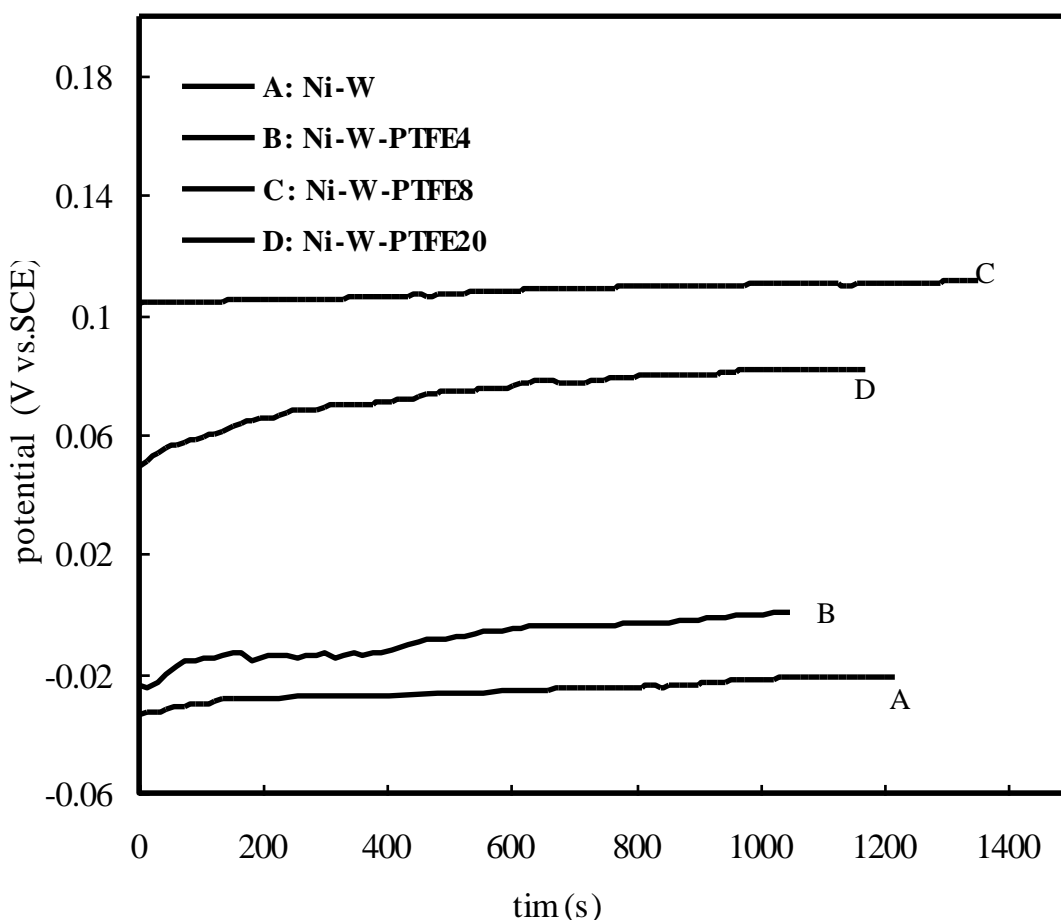
Figure 9. Open-circuit polarization potential vs. time in 3.5% NaCl solution of Ni-W-PTFE nanocomposite coatings.
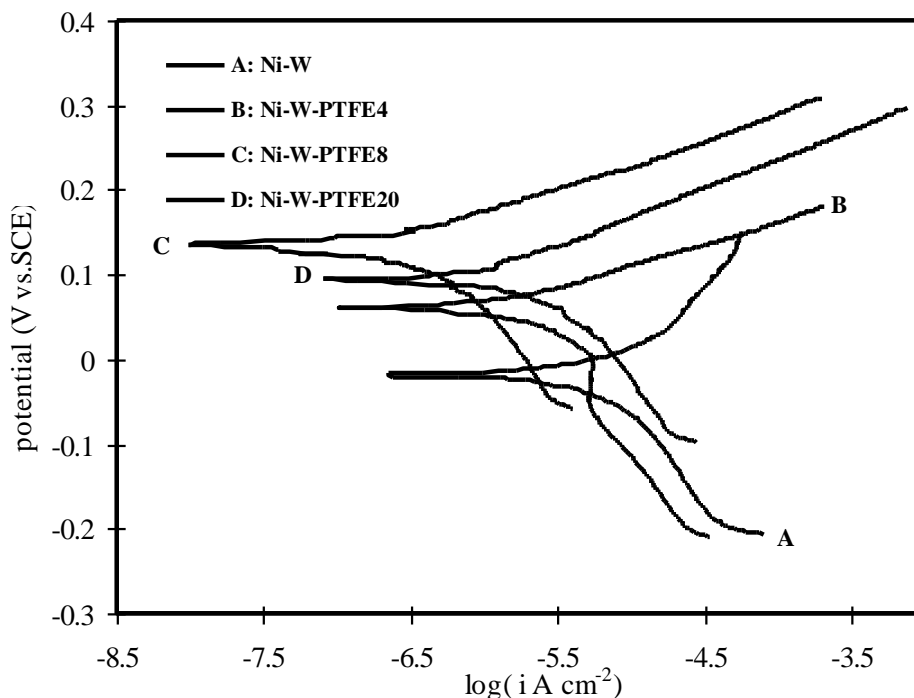
Figure 10. Potentiodynamic polarization graphs (at scan rate of 0.2 mV s^{-1}) in 3.5% NaCl solution of Ni-W/PTFE nanocomposite coatings.

**Table 3.** The values of E$_{corr}$ and i$_{corr}$ of Ni-W-PTFE nanocomposite coatings in 3.5 wt. % NaCl solution

Sample	E$_{corr}$ (mV)	i$_{corr}$ (μA cm^{-2})
Ni-W-PTFE (0 g l^{-1})	-11.23	50
Ni-W-PTFE (4 g l^{-1})	61.79	8
Ni-W-PTFE (8 g l^{-1})	135.47	0.15
Ni-W-PTFE (20 g l^{-1})	93.87	1

The second method is Electrical Impedance Spectroscopy (EIS) method that has been used for electrochemical behavior of coating in 3.5% of NaCl solution. The typical Nyquist and bode plots of the nano composite in different conditions have been illustrated in Fig.11 and Fig.12 respectively.

Single semicircular arc have been obtained in the Nyquist plots for Ni-W-PTFE nanocomposite films in the investigated frequency region. As shown in Fig. 11, Nyquist arc radius is increased when the PTFE concentration in the nanocomposite coatings increased and this indicates the better anticorrosion property of these compositions. The equivalent circuit of coatings was also shown inset of the Fig.11. The fitting results for the films are listed in Table 4. The higher arc indicates higher charge transfer resistant. Lower effective metallic surface area in the nanocomposite films is one of the main reasons for this improvement in charge transfer resistant and as a consequence more corrosion resistant behavior. The EIS results also confirm the potentiodynamic polarization results.
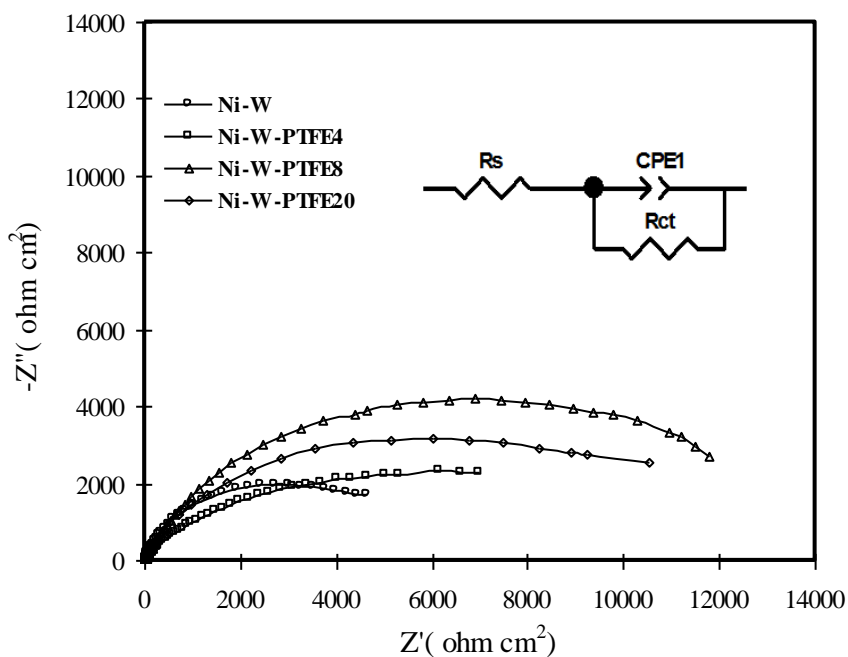
Figure 11. Equivalent circuit and Nyquist plots of Ni-W-PTFE composite coatings in 3.5 wt. % NaCl solution for different PTFE nanoparticle concentrations.
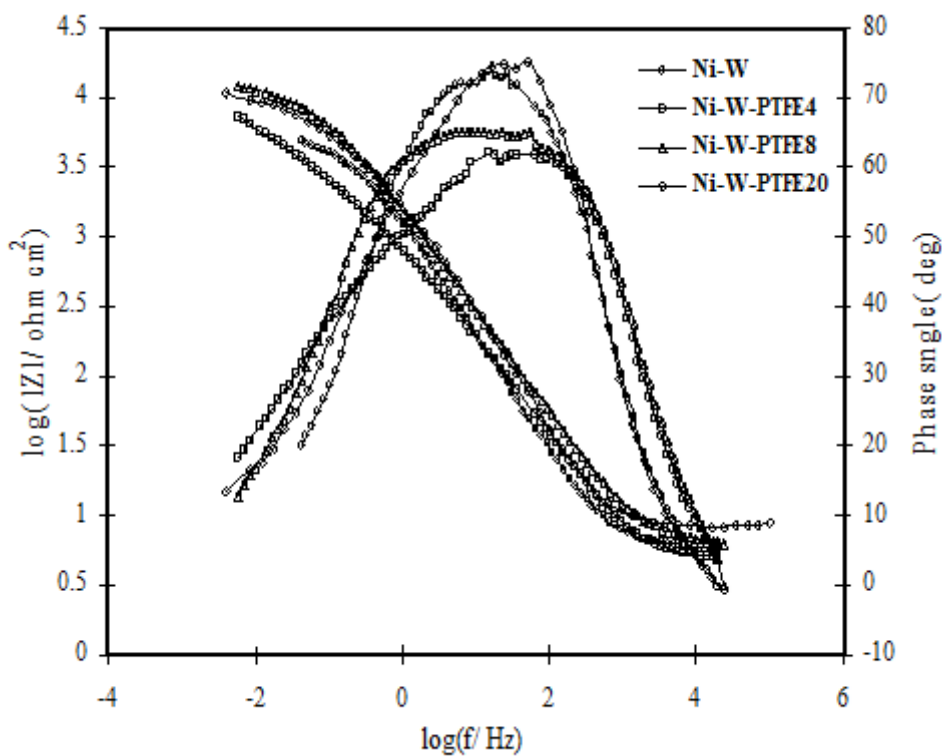
Figure 12. Bode-phase plots of Ni-W-PTFE composite coatings in 3.5 wt. % NaCl solution for different PTFE nanoparticle concentrations.

.

The maximum charge transfer resistant (R_{ct}) value was obtained for the 8 gl^{-1} of PTFE composite coating of Ni-W-PTFE. The PTFE nanoparticles addition in the composite coating has reduced the capacitance of the double layer values. These properties may improve the coating compactness and decrease diffusion of the corrosive species into the coating and contributing to the better electrochemical performance. According to the XRD results the nanocomposite coating with 8 gl^{-1} has smallest crystalline size. Also the AFM and SEM image show that this condition has a best surface homogeneity. As a consequence, it can be said that low grain size has a higher fraction of passive layer and low corrosion rate due to the high density of nucleation sites for passive film [24]. The low corrosion resistant in high concentration of PTFE (20 gl^{-1}) can be explained according to Yi-Hui You et al [8] research. They claim that the high concentration of PTFE, could be attributed to the inter-granular corrosion taking place at the crystal boundaries and addition of more PTFE, leads to highly sheet-like crystalline nature in the deposition. The electrochemical results show that, Ni-W-PTFE composite coating that was deposited in the presence of 8 g1^{-1} PTFE nanoparticles provided the optimum corrosion performance among the other investigated coatings, which improved the corrosion resistance with the inhibition efficiency by approximately 95%.

Table 4. Fitting results of the impedance spectra of Ni-W-PTFE composite coatings in 3.5 wt.% NaCl solution.

Coating	PTFE (0g 1^{-1})	PTFE (4 g 1^{-1})	PTFE (8 g 1^{-1})	PTFE (20 g 1^{-1})
R_s (Ω cm^2)	5.71	7.2	5.9	6.9
CPE_1-T(F. cm^2)	13.2 *10^{-5}	12.1 *10^{-5}	10.4 *10^{-5}	11.9 *10^{-5}
CPE1-P	0.81	0.83	0.89	0.83
R_{ct} (Ω cm^2)	6278	7500	12760	6395
Error(%)	0.004	0.003	0.003	0.003

4. CONCLUSION

The Ni-W-PTFE nanocomposite coatings were successfully prepared from tartrate electrolyte. The structural, nano-tribological and electrochemical performances of the nanocomposite coatings were evaluated. Results showed that the PTFE particles significantly changed the structure and morphology of the deposited coating and decreased the nodules and crystalline size. The coatings with 8 g 1^{-1} PTFE shows the low friction force in comparison with other samples. Charge transfer and corrosion resistant of the Ni-W coating was improved by co-deposition of the PTFE particles. The optimum condition was obtained in 8gl^{-1} PTFE concentration in electrolyte.

References

1. A. Stankiewicz, J. Masalski, B. Szczygieł, *Mat. Corr.*, 64 (2013) 908
2. A. Farzaneh, M. Mohammadi, M. Ehteshamzadeh, F. Mohammadi, *Appl. Surf. Sci.*, 276 (2013) 697
3. M. Hosseini, M. Abdolmaleki, J. Ghahremani, *Corr. Eng., Sci. Technol.,* 49 (2014) 247
4. M. Hosseini, M. Abdolmaleki, S. Seyed Sadjadi, M. Raghibi Boroujeni, M. Arshadi, H. Khoshvaght, *Surf. Eng.,* 25 (2009) 382

5. A.F.a.B.J.A.A. Zaki Ahmad, in: Z. Ahmad (Ed.) Recent Trends in Processing and Degradation of Aluminium Alloys, InTech**2011**.
6. B. Bakhit, A. Akbari, F. Nasirpouri, M.G. Hosseini, *App. Surf. Sci.,* 307 (2014) 351
7. F. Nasirpouri, M. Sanaeian, A. Samardak, E. Sukovatitsina, A. Ognev, L. Chebotkevich, M.-G. Hosseini ,M. Abdolmaleki, *Appl. Surf. Sci*., 292 (2014) 795
8. Y.-H. You, C.-D. Gu, X.-L. Wang, J.-P. Tu, *Int. J. Electrochem. Sci.,* 7 (2012) 12440
9. M. Mohammadi, M. Ghorbani, *J. coat. technol. res.,* 8 (2011) 527
10. M. Mohammadi ,M. Ghorbani, A. Azizi, *J. coat. technol. res*., 7 (2010) 697
11. Z. Guo, X. Zhu, R. Xu, *Mat. scie. technol.,* 20 (2004) 257
12. B. Szeptycka, A. Gajewska-MidziaIek, *Rev. Adv. Mater. Sci.,* 14 (2007) 135
13. Z. Guo, R .Xu, X. Zhu, *Surf. Coat. Technol.,* 187 (2004)141
14. F. Wang, S. Arai, M. Endo, *Mat. trans.,* 45 (2004) 1311
15. M. Cardinal, P. Castro, J. Baxi, H. Liang, F. Williams, *Surf. Coat. Technol.,* 204 (2009) 85
16. M. Hosseini, M. Abdolmaleki, S. Ashrafpoor, R. Najjar, *Surf. Coat. Technol*., 206 (2012) 4546
17. A. Farzaneh, M. Ehteshamzadeh, M. Ghorbani, J.V. Mehrabani, *J. Coat. Technol. Res*., 7 (2010) 547
18. A. Farzaneh, M. Ehteshamzadeh, M. Mohammadi, J. *Appl. Electrochem*., 41 (2011) 19
19. S. Aruna, P. Lashmi, H. Seema, *RSC Advances*, in press.
20. I. Tudela, Y. Zhang, M. Pal, I. Kerr, T.J. Mason, A.J. Cobley, *Surf. Coat. Technol*., 264 (2015) 49
21. Y .Wu, L. Liu, B. Shen, W. Hu, *J. mat.science,* 40 (2005) 5057
22. Y. Wang, Q. Zhou, K. Li, Q. Zhong, Q.B. Bui, *Ceram. Inter.,* 41 (2015) 7
23. S. Sangeetha, G.P. Kalaignan, J.T. Anthuvan, *Appl. Surf. Sci*., 359 (2015) 412
24. S. Sangeetha, G.P. Kalaignan, *RSC Adv*., 5 (2015) 74115